J. Bangladesh Acad. Sci. 47(2); 267-275: December 2023 DOI:https://doi.org/10.3329/jbas.v47i2.66872

Journal of Bangladesh Academy of Sciences

Journal homepage: http://www.bas.org.bd/publications/jbas.html

Research Article

Speciation of Cr(III) and Cr(VI) in aqueous solution and their removal by oyster mushroom biomass

M. N. M. Asif, Rashedul Islam, M. A. Goni[1], Sumon Ganguli[2], Ashok Kumar Chakraborty[3],
Mahbub Kabir, and Md Abdus Sabur[*]

Department of Chemistry, Jahangirnagar University, Savar, Dhaka, Bangladesh

ARTICLE INFO

Article History

Received: 13 June 2023
Revised: 12 November 2023
Accepted: 14 November 2023

Keywords: Biosorption, Chromium removal, Adsorption isotherms, pH envelope.

ABSTRACT

This study investigates the effectiveness of oyster mushroom (*Pleurotus platypus*) for the removal of Cr(III) and Cr(VI) from aqueous solutions by conducting a series of batch adsorption experiments. Results from the adsorption pH envelope experiments show that while the adsorption of Cr(III) increases with increasing pH, the adsorption of Cr(VI) decreases as the pH rises. These two distinct pH envelope patterns for Cr(III) and Cr(VI) suggest that the adsorption processes are primarily driven by the electrostatic force of attractions followed by the ligand exchange process. Findings from the adsorption isotherm experiments demonstrate that chromium binding to the adsorbent surface is better described by the Freundlich model than the Langmuir model, underscoring the presence of multiple surface binding sites. The study highlights the significance of identifying dominant chromium species before they are subjected to adsorptive removal from contaminated waters.

Introduction

Heavy metals generally enter natural environments (e.g., water and soil) by weathering rocks and minerals (Bradl, 2005; Finlay et al., 2019). Nevertheless, anthropogenic activities including mining, smelting, combustion of fossil fuel, and the improper discharge of untreated industrial wastes can lead to excessive metal presence in various environmental compartments (Bradl, 2005; Wuana and Okieimen, 2011). Once heavy metals enter natural systems, the system's recovery becomes challenging, often relying on natural attenuation for restoration. Generally, organic and inorganic wastes often contaminate natural environments near industrial sites (Khan et al., 2011; Rahman et al., 2014). Therefore, reusing treated water is another option for reducing environmental pollution.

Conventional water treatment methods commonly used to remove heavy metals from contaminated waters include reverse osmosis, ion exchange, membrane filtration, electro-dialysis etc. (Azimi et al., 2017; Carolin et al., 2017). While ion exchange and membrane filtration methods are highly effective, they are costly and often impractical for commercial use. An alternative approach is the coagulation-precipitation method, which can effectively remove organic and inorganic pollutants from contaminated water. This method offers relative affordability and ease of design but may generate a substantial volume of sludge. Additionally, metal ions from contaminated waters can be successfully removed by adsorption filtration techniques (Bhatnagar and Sillanpää, 2010; Bhatti et al., 2007; Kumari et al., 2006; Nuhoglu et al., 2002; Reddy et al., 2011, 2010; Say et al., 2001; Vimala and Das, 2009).

---

[*] Corresponding author: <sabur@juniv.edu>

[1] *Department of Chemistry, Bangladesh University of Engineering and Technology, Dhaka, Bangladesh*

[2] *Department of Applied Chemistry and Chemical Engineering, University of Chittagong, Chittagong, Bangladesh*

[3] *Department of Applied Chemistry and Chemical Engineering, Islamic University, Khustia, Bangladesh*

Besides the typical chemical adsorption methods, biosorption has emerged as an attractive and viable alternative for mitigating environmental pollution from industrial wastewater (Alluri et al., 2007; Bhatnagar and Sillanpää, 2010; Kanamarlapudi et al., 2018; Say et al., 2001). Typical biosorbents consist of lignin, cellulose, and proteins with various surface functional groups such as hydroxyl, carboxyl, and amide (Shakoor et al., 2019). The presence of these functional groups on the surface of biological materials determines the potential binding capacity of biosorbents with a wide range of chemical contaminants, including cations and anions. Over the past two decades, numerous biosorbents have been investigated for their effectiveness in the removal of heavy metals from aqueous wastes (Alluri et al., 2007; Bhatnagar and Sillanpää, 2010; Kanamarlapudi et al., 2018; Say et al., 2001). Compared to other biosorbents, mushroom powder has demonstrated promise and effectiveness in removing pollutants from diverse sources (Das, 2005; Mathialagan et al., 2003; Prasad and Sachin, 2013; Vimala and Das, 2009).

Previous studies have extensively examined the capabilities of common biosorbents in removing chromium and other heavy metals (Gupta et al., 2011; Kanamarlapudi et al., 2018; Michalak et al., 2013; Sag and Kutsal, 2001; Vimala and Das, 2009). However, mechanisms governing the binding of both cationic and anionic chromium to the mushroom surface remain relatively unexplored (Chen et al., 2005; Das, 2005; Ertugay and Bayhan, 2008; Jing et al., 2011; Kanamarlapudi et al., 2018; Suseem and Mary Saral, 2014). Here, we use ground mushroom biomass to evaluate the potential mechanisms and optimal conditions for the adsorptive removal of Cr(III) and Cr(VI) using batch adsorption experiments. This study highlights the significance of understanding chromium speciation before their adsorptive removal from contaminated waters.

Materials and Methods

Preparation of biosorbent

Fruit bodies of oyster mushrooms (*Pleurotus platypus*) were collected from the National Mushroom Development and Extension Centre, Savar, Bangladesh. Mushrooms were washed thoroughly with deionized water to remove the dirt and other undesirable materials. Subsequently, the mushrooms were turned into smaller pieces and dried in an oven at 80 °C for 24 h. After drying, the fruit bodies were finely ground using a mortar and pestle.

Preparation of stock solution

Individual stock solutions of 1000 mM of Cr(III) and Cr(VI) were prepared separately by dissolving the solid powder of $CrCl_3$ (Merck, India, 158.35 g/mol) and $K_2Cr_2O_7$ (Guangdong Guanghua Chemical Factory Co, Ltd, China, 294.185 g/mol), respectively, in deionized water. The solutions were subsequently diluted to the appropriate concentrations based on the type of adsorption experiments.

Adsorption experiment

Batch adsorption experiments were conducted in Cr(III) or Cr(VI) solutions containing solid mushroom powder at 28±1°C on an orbital shaker. The effect of pH on the adsorption of chromium to adsorbent was investigated within the pH range from 2.0 to 8.0. Before starting the adsorption pH envelope experiment, pH in the chromium solutions (0.2 mM) was adjusted between pH 2.0 and 8.0 using HCl and NaOH solutions. The chromium solutions (100 mL each) with suitable pH adjustment were then equilibrated separately with the adsorbent (1.0 g/L) for 6 h in reagent bottles.

Kinetic studies for the adsorption of chromium with the adsorbent were conducted. Solutions of both chromium species (0.2 mM each) were agitated with the adsorbent (1.0 g/L) in six individual reactors. This experiment's initial pH (before adsorption) was adjusted separately for each chromium species based on the maximum adsorption pH condition, as revealed from the adsorption pH envelope experiment. The reactors were sacrificially removed at 10, 20, 30, 60, 120, 180, 240, and 300 min, respectively.

The effects of initial chromium concentrations (0.2 to 2 mM) for chromium adsorption on the mushroom surface were conducted for 180 min. The initial pH levels (before adsorption) for assessing the effect of adsorbent dosages and the initial concentrations were adjusted separately based on the maximum adsorption pH condition obtained from the pH envelope and adsorption kinetic studies.

After the adsorption experiments, the suspension samples from each reactor were filtered using 0.45 µM (Whatman) filter paper, and the filtrate was stored at 4 °C until analysis. Chromium concentrations in the samples were determined using atomic absorption spectroscopy before and after each adsorption experiment (AA-7000, Shimadzu, Japan) equipped with air acetylene flame. The adsorption data are presented in terms of surface coverage and removal percentage. The surface coverage (θ) by Cr(III) and Cr(VI) is estimated from the difference between the initial (C_0) and final (Ce) concentration of chromium and the amount of adsorbent (in grams) used in the adsorption experiments.

Results and discussion

Adsorption pH envelope

The effect of initial pH (before adsorption) on the adsorption of both Cr(III) and Cr(VI) onto the mushroom surface was evaluated within the pH range of 2.0 to 8.0. pH plays a vital role in determining the degree of ionization of sorbates, influencing the speciation of sorbent surfaces, and affecting the solubility of metal ions (Langmuir, 1997; Michalak et al., 2013). For instance, the adsorption of anions generally decreases with increasing pH, although the adsorption pH envelope depends on the sorbent's point of zero charge (PZC). Conversely, the adsorption characteristics of cations grow with increasing solution pH (Langmuir, 1997; Sabur, 2019). The calculation of aqueous speciation for Cr(III) and Cr(VI) relies on the reactions and their respective constants listed in Table 1, which are comparable to those documented in existing literature (Papassiopi et al., 2014; Szabó et al., 2018). Aqueous speciation of Cr(III) and Cr(VI) are computed by PHREEQC 3 (Parkhurst and Appelo, 2013) with the minteq.dat database (Fig. 1).

Table 1. Cr(III) and Cr(VI) speciation reactions and the corresponding reaction constants at 25 °C used to construct Fig. 1.

Species	Reaction	logK
Cr(III)	$Cr(OH)_2+ + 2H+ = Cr^{3+} + 2H_2O$	9.84
	$Cr(OH)_2^{+} + H+ = Cr(OH)^{2+} + H_2O$	6.27
	$Cr(OH)^{2+} + H_2O = Cr(OH)_3 + H+$	-7.36
	$Cr(OH)^{2+} + 2H2O = Cr(OH)4- + 2H+$	-16.18
	$Cr(OH)^{2+} = CrO2- + 2H+$	-17.74
Cr(VI)	$CrO_4^{2-} + H^{+} = HCrO^{4-}$	6.51
	$CrO4^{2-} + 2H^{+} = H_2CrO_4$	5.65
	$2CrO4^{2-} + 2H^{+} = Cr_2O_7^{2-} + H_2O$	14.56

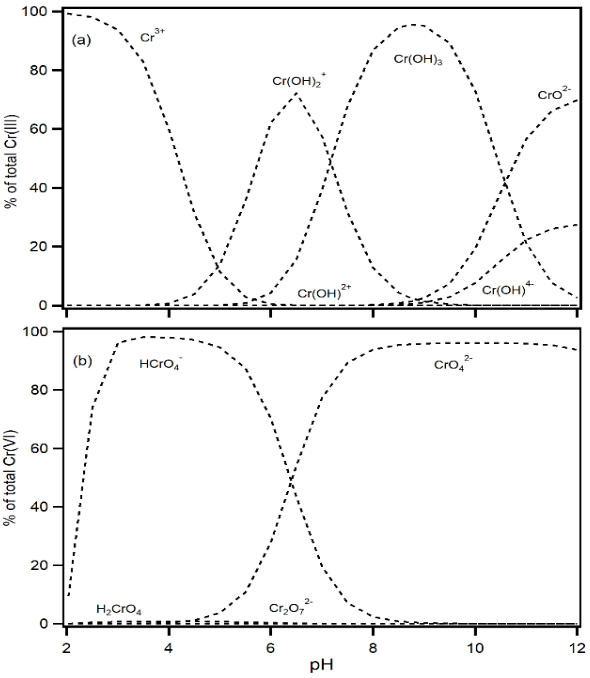

Fig. 1. The speciation of Cr(III) (a) and Cr(VI) (b) in aqueous solutions as a function of pH at 25°C. The speciation diagrams were constructed using 0.2 mM solutions of $CrCl_3$ and K_2CrO_7 for Cr(III) and Cr(VI), respectively. The diagrams were generated with the PHREEQC 3 computer program, incorporating reaction constants from the minteq.dat database, consistent with previous studies (Papassiopi et al., 2014; Szabó et al., 2018).

In an aqueous solution of $CrCl_3$, Cr^{3+} undergoes hydrolysis, and the hydrolytic products of chromium mostly exist as cations within the pH range of 2.0 to 8.0 (Fig. 1a). However, under alkaline conditions, typically above pH 8.0, the hydrolyzed product of Cr^{3+} transforms into negatively charged $Cr(OH)^{4-}$. When potassium dichromate ($K_2Cr_2O_7$) is dissolved in water, it forms several stable ions (Fig. 1b) contingent upon the concentration and pH in the solution. Notably, $HCrO_4^-$ predominates under acidic conditions, while CrO_4^{2-} prevails under alkaline conditions. $K_2Cr_2O_7$ can also generate $Cr_2O_7^{2-}$, however, the presence of this ion may be insignificant in our experimental system based on the concentration range used in the adsorption pH envelope experiments.

Fig. 2 shows the results of the adsorption pH isotherm studies reveal that the adsorption of chromium (III) on mushroom surface increases as the initial pH of the solution rises (Fig. 2). A similar adsorption isotherm pattern was found in the adsorption of Cr(III) on lichen biomass (Uluozlu et al., 2008) and is consistent with the adsorption of other metal cations on mushroom surface (Ertugay and Bayhan, 2010; Vimala and Das, 2009). Cr(III) ions exist primarily as positively charged ions with free Cr^{3+} ions or as hydrated Cr^{3+} ions with coordinated hydroxyl groups (OH^-) in aqueous solutions. Therefore, the speciation of the Cr(III) ion changes with the variation of pH in the solutions due to the changing coordination states of the metal ion (Fig. 1b). Increasing pH (e.g., increasing OH^- ion concentration) in the solution initially results in the neutralization of the positive charge carried by the Cr^{3+} ion. Subsequent rise of pH results in the negative charge buildup on the metal ion, primarily due to the binding of negatively charged OH^- groups.

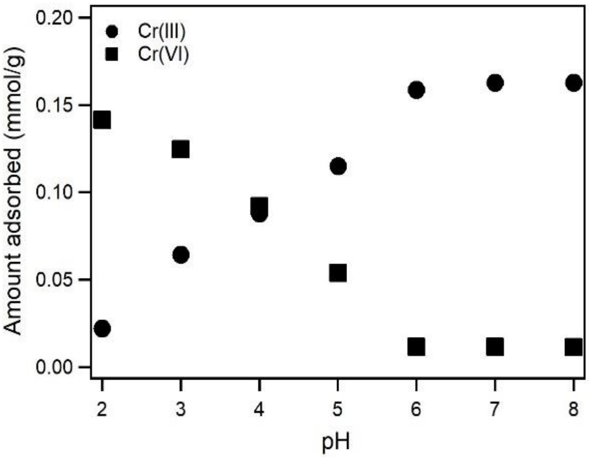

Fig. 2. Effect of pH on Cr(III) and Cr(VI) adsorption on the mushroom surface.

The predominant functional groups found in the typical biosorbents are hydroxyl, carboxylic acid, and amide (Shakoor et al., 2019). These functional groups at the surface may undergo acid-base reactions and can transform the biosorbent's surfaces with a negative charge under alkaline conditions (Michalak et al., 2013). The positively charged Cr(III) ions experience a greater electrostatic attraction with the solid surface, and this attraction increases with increasing pH, enhancing Cr(III) removal from the aqueous solution. Apart from the adsorptive removal of cationic chromium species, chromium removal from the aqueous phase might also occur via Cr(OH)3 precipitation on the adsorbent surface (Guimarães et al., 2020). The later process will likely be thermodynamically favorable at near neutral to alkaline conditions with increasing solution pH, e.g., pH > 6.0 (Fig. 1a).

The maximum adsorption for Cr(VI) was observed under strongly acidic conditions, followed by a sharp decline as the pH increased further (Fig. 2). This trend is consistent with prior research, including studies involving surfactant-modified mushroom and other biosorbents (Fernández-López et al., 2014; Jing et al., 2011). Additionally, Cr(VI) adsorption becomes minimal at or above a pH of approximately 6.0. This phenomenon can be elucidated by the fact that Cr(VI) primarily exists as negatively charged chromate ions ($HCrO_4^-$ and CrO_4^{2-}) under the specified experimental conditions (Fig. 1b).

As the pH shifts from acidic to alkaline conditions, there is a notable increase in the concentration of singly deprotonated chromate species ($HCrO_4^-$), leading to the formation of CrO_4^{2-} (Fig. 1b). Therefore, the limited adsorption Cr(VI) at or above the pH 6.0 suggest that the adsorption of $HCrO_4^-$ on the mushroom surface primarily occurred from pH 2.0 to 6.0. The sharp decrease of Cr(VI) adsorption with further pH elevation beyond 6.0 implies that the mushroom surface undergoes a negative charge modification, likely attributed to either the deprotonation of the surface-active groups or the adsorption of hydroxyl (OH^-) groups onto the solid surface. These findings collectively suggest that an increase in solution pH leads to the deduction in electrostatic attraction between the deprotonated chromate ion (CrO_4^{2-}) and the negatively charged surface, resulting in diminished Cr(VI) adsorption onto the solid surface.

Effect of equilibrium time

Kinetic studies for the adsorption of Cr(III) and Cr(VI) are conducted using identical concentrations (0.2 mM each) and fixed chromium solution volume (100 mL). The amount of adsorbent also remained the same, with the only variation being the pH levels, set at 6.5 and 2.0 for Cr(III) and 2.0 for Cr(VI). Results show that the adsorption of Cr(III) and Cr(VI) progressively increases as the equilibration time lengthens (Fig. 3). The removal of chromium occurs rapidly, mostly within 100 min of the adsorption period. This rapid adsorption may be attributed to the higher availability of surface binding sites on the biomass. However, the adsorption rate gradually diminishes as the equilibration time extends. This deceleration in adsorption suggests a potential depletion of surface-active sites due to the continued adsorption process.

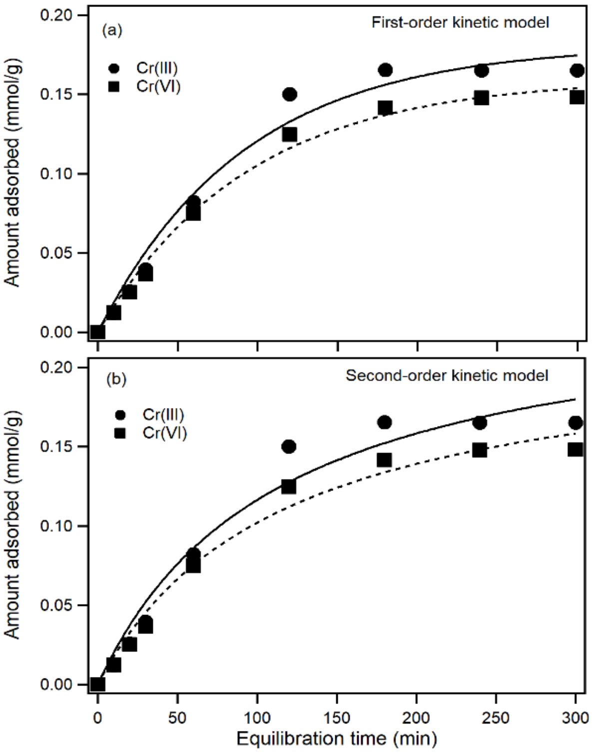

Fig. 3. The kinetic data (symbol) for the adsorption of Cr(III) and Cr(VI) on the mushroom surface. The dotted solid and dotted lines represent simulated kinetic data for Cr(III) and Cr(VI), respectively, according to the pseudo-first-order (a) and second-order (b) kinetic models.

Adsorption kinetic data are often fitted to first and second-order kinetic models to gain insights into the adsorption mechanism. Kinetic parameters for the adsorption of Cr(III) and Cr(VI) are extracted by fitting the experimental data using first and second-order adsorption kinetic models. The mathematical representation of pseudo first and second-order adsorption kinetics (Lima et al., 2015) can be expressed by Equation 1 and Equation 2.

$$\theta(t) = \theta(1 - e^{-k_1 . t}) \ldots\ldots\ldots\ldots\ldots\ldots\ldots\ldots\ldots\ldots\ldots \quad (1)$$

$$\theta(t) = \frac{k_2 \theta t}{1 + k\theta t} \ldots\ldots\ldots\ldots\ldots\ldots\ldots\ldots\ldots\ldots\ldots\ldots \quad (2)$$

Where, $\theta(t)$ is the amount of Cr(III), or Cr(VI) sorbed onto the adsorbent surface (in mmol/g) at time t (h) with rate constants k_1 and k_2 for the first and second-order adsorption models, respectively.

Table 2. Kinetic parameters were extracted for the adsorption of Cr(III) (at pH 2.0) and Cr(VI) (at pH 6.5) by fitting the experimental data to Equation 1 and 2 with a 95% confidence limit. Chi-square (χ2) values illustrate the quality of the fit.

First-order			
Species	**θ (mmol/g)**	***k*** **(h^{-1})**	χ^2
Cr(III)	0.18±0.03	0.01±0.00	$7.83{\pm}10^{-4}$
Cr(VI)	0.16±0.01	0.01±0.00	$2.35{\pm}10^{-4}$
Second-order			
Species	**θ (mmol/g)**	***k*** **g/(mmol×h)**	χ^2
Cr(III)	0.25 ± 0.07	0.04 ± 0.03	$1.27{\pm}10^{-3}$
Cr(VI)	0.22 ± 0.04	0.04 ± 0.03	$4.88{\pm}10^{-3}$

Table 2 shows that the θ_1 values derived from the pseudo-first-order kinetic model for Cr(III) and Cr(VI) adsorption are aligned closely with the data point obtained at or near the equilibrium. Notably, the pseudo-second-order adsorption kinetic model estimates slightly higher θ_1 values than the measured values (Table 2). Furthermore, the pseudo-first-order kinetic model better fits the experimental data than the pseudo-second-order adsorption kinetic model, as evident from the respective chi-square values.

This result indicates the importance of available active sites on the adsorbent surface for binding both chromium species.

Effect of initial concentration

The initial concentration of sorbate, the adsorbent, and sorbate-to-adsorbent ratios play a significant role in shaping adsorption isotherm. The surface coverage increases with sorbate concentration for a given amount of sorbent. Adsorption mechanisms and the binding strength of surface species are often described in terms of Langmuir and Freundlich models (Lima et al., 2015). The Langmuir model assumes the homogeneous distribution of the surface-active sites by sorbate species, whereas the Freundlich predicts the heterogamous distribution of potentially active sites on surfaces (Lima et al., 2015). Equations 3 and 4 represent the mathematical models describing the nonlinear Langmuir and Freundlich adsorption isotherms (Langmuir, 1997; Lima et al., 2015) can be shown by Equations 3 and 4.

$$\theta = \theta_{max}\frac{K_L[A]}{1 + K_L[A]} \ldots\ldots\ldots\ldots\ldots\ldots\ldots\ldots\ldots\ldots\ldots\ldots \quad (3)$$

$$\theta = K_F * [A]^{1/n} \ldots\ldots\ldots\ldots\ldots\ldots\ldots\ldots\ldots\ldots\ldots\ldots\ldots\ldots \quad (4)$$

Where, θ in Equations 3 and 4 represents the quantity of chromium adsorbed onto the adsorbent surface (mmol/g) at a specific chromium concentration of $[A]$ and θ_{max} in Equation 3 is the maximum surface coverage of mushroom biomass by chromium. K_L and K_F denote the Langmuir and Freundlich adsorption constants, while 'n' in Equation 4 stands for the order of the surface reaction.

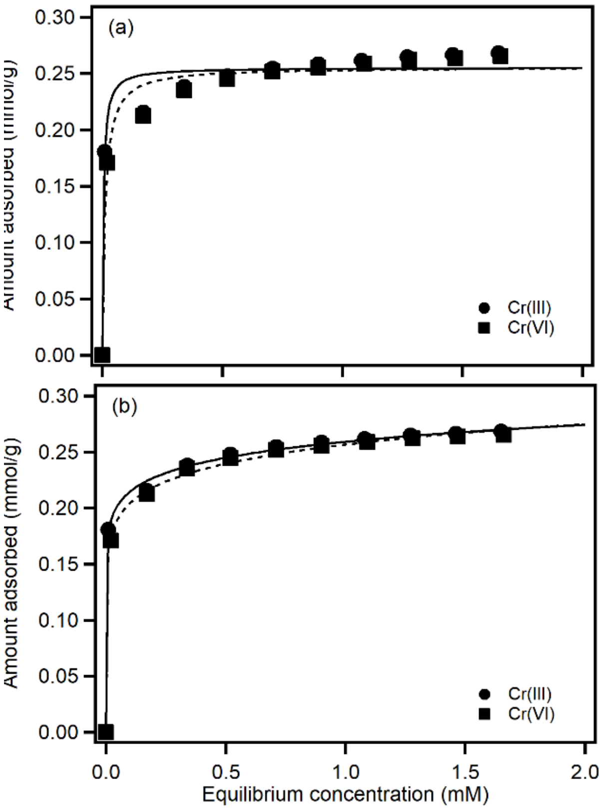

Fig. 4. Effect of initial concentration on removing Cr(III) and Cr(VI) by mushrooms. Experimental data and the predictions by Langmuir (a) and Freundlich (b) models are shown by the markers and dotted lines, respectively.

Experimental data in Fig. 4 shows that the adsorption of Cr (III) and Cr (VI) ions strongly influenced their initial concentrations. As observed in Fig. 4, the adsorption of chromium increases with rising initial chromium concentrations (Fig. 4), reaching a plateau near 0.5 mM of chromium, as anticipated. The experimental data are fitted to the Langmuir and Freundlich adsorption models in Fig. 4a and 4b, respectively, and the resulting adsorption isotherm parameters are presented in Table 3.

By comparing least square fits (chi-square values) for the experimental data, it is evident that the Freundlich adsorption model better fits the experimental data than the Langmuir model. However, the adsorption constant obtained by fitting the experimental data using the Langmuir and Freundlich models greatly depends on the experimental conditions. This implies that the values of K_L and K_F obtained from the present study cannot be compared with adsorption processes involving Cr(III) or Cr(VI) on different biosorbents, nor are they applicable to various other sorbates (e.g., lead, cadmium, arsenic, etc.) when considering the mushroom surface as the adsorbent. Even these values cannot be directly compared to the adsorption processes of Cr(III) or Cr(VI) on the same mushroom surface under different pH conditions. Notably, the values of K_L are similar for both Cr(III) and Cr(VI) adsorptions, accounting for the respective error bars (Table 3). This result indicates that the adsorption of Cr(III) and Cr(VI) to the mushroom surface occurs with similar chromium binding strengths, also reflected in K_F values (Table 3).

As discussed earlier, the values of reaction quotients for the adsorption of Cr(III) or Cr(VI) obtained by the two different adsorption models cannot be compared, but the respective chi-square values can demonstrate the relative performance of the models to explain the experimental data. Thus, the significance of adsorption constants (K_L and K_F) for comparing the binding strength of Cr(III) and Cr(VI) with the mushroom surface is limited, primarily because the adsorption isotherm experiments are conducted under distinct pH conditions. Nonetheless, the potential binding mechanisms can be partially elucidated for the adsorption of both Cr(III) or Cr(VI) by comparing the corresponding K_L and K_F values derived from the Langmuir and Freundlich models. Compared to the Langmuir model, the lower chi-square values obtained from fitting experimental data with the Freundlich model suggest that mushroom powder will likely provide multiple surface-active sites for adsorbing chromium species from aqueous solutions. The potential diffusion of chromium from the mushroom surfaces to the interior of the soil is also possible.

Table 3. Adsorption isotherm parameters were extracted by fitting the experimental data to the Langmuir (Equation 3) and Freundlich (Equation 4) adsorption models, respectively. The chi-square values (χ_c^2 = 4.87) represent the goodness of fit.

Langmuir model			
	K_L	θ_{max}	χ^2
Cr(III)	224±14	0.26±0.01	1.85×10^{-3}
Cr(VI)	88±43	0.26±0.00	1.31×10^{-3}
Freundlich model			
	K_F	n	χ^2
Cr(III)	0.26±0.00	12.22±1.25	1.03×10^{-4}
Cr(VI)	0.26±0.00	10.08±0.98	1.05×10^{-4}

Conclusion

Here, we evaluate mushroom surfaces' adsorption behavior for removing Cr(III) and Cr(VI) from aqueous solutions. The results from the pH envelope studies show that Cr(III) and Cr(VI) adsorption occur with two distinct pH envelope patterns. While anionic Cr(VI) removal is favored under acidic conditions, the maximum cationic Cr(III) removal occurs under alkaline conditions. These results indicate that removing aqueous chromium is primarily driven by the electrostatic attraction between the sorbate ions and the active functional groups on the adsorbent surface, followed by the surface complexation reactions. Adsorption isotherm studies for both chromium species show that the experimental data align better with the Freundlich model than the Langmuir model. This result implies that mushroom surfaces possess multiple active sites for binding cationic and anionic chromium species. Therefore, mushroom powders hold potential as a low-cost adsorbent for removing chromium from contaminated waters with a prior understanding of the oxidation states of dissolved chromium.

Acknowledgments

The authors are grateful to the Wazed Miah Science Research Centre, Jahangirnagar University, Savar, Dhaka, for providing the analytical facility with the atomic absorption spectroscopy.

Disclosure statement

The authors do not have any conflict of interest regarding the publication of this manuscript.

References

Alluri HK, Ronda SR, Settalluri VS, Bondili JS, Suryanarayana V and Venkateshwar P. Biosorption: An eco-friendly alternative for heavy metal removal. *Afr. J. Biotechnol.* 2007; 6(25): 2924-2931.

Azimi A, Azari A, Rezakazemi M and Ansarpour M. Removal of heavy metals from industrial wastewaters: a review.*Chem.Bio.Eng. Rev*. 2017; 4(1): 37-59.

Bhatnagar Amit and Sillanpää M. Utilization of agro-industrial and municipal waste materials as potential adsorbents for water treatment-A review. *Chem. Eng. J.* 2010; 157(2-3): 277-296.

Bhatti HN, Mumtaz B, Hanif MA and Nadeem R. Removal of Zn(II) ions from aqueous solution using Moringa oleifera Lam. (horseradish tree) biomass. *Process Biochem*. 2007; 42(4): 547-553.

Bradl HB. 2005. Sources and origins of heavy metals. In: Interface Science and Technology. Elsevier. 2005; p.1-7.

Carolin CF, Kumar PS, Saravanan A, Joshiba GJ and Naushad M. Efficient techniques for the removal of toxic heavy metals from aquatic environment: A review. *J. Environ. Chem. Eng*. 2017; 5(3): 2782-2799.

Chen GQ, Zeng GM, Tu X, Huang GH and Chen YN. A novel biosorbent: characterization of the spent mushroom compost and its application for removal of heavy metals. J. Environ. Sci. 2005; 17(5): 756-760.

Das N. Heavy metals biosorption by mushrooms. *Nat. Prod. Radiance.* 2005; 4: 454-459.

Ertugay N and Bayhan YK. Biosorption of Cr (VI) from aqueous solutions by biomass of Agaricus bisporus. *J. Hazard. Mater.* 2008; 154(1-3): 432-439.

Ertugay N and Bayhan YK. The removal of copper (II) ion by using mushroom biomass (Agaricus bisporus) and kinetic modelling. *Desalination* 2010; 255(1-3): 137-142.

Fernández-López JA, Angosto JM and Avilés MD. Biosorption of hexavalent chromium from aqueous medium with opuntia biomass. *Sci. World J.* 2014; ID 670249: 1-8.

Finlay RD, Mahmood S, Rosenstock N, Bolou-Bi EB, Köhler SJ, Fahad Z, Rosling A, Wallander H, Belyazid S, Bishop K and Lian B. Biological weathering and its consequences at different spatial levels–from nanoscale to global scale. *Biogeosciences* 2020; 17(6): 1507-1533.

Guimarães T, Paquini LD, Ferraz BRL, Profeti LPR and Profeti D. Efficient removal of Cu (II) and Cr (III) contaminants from aqueous solutions using marble waste powder. *J. Environ. Chem. Eng.* 2020; 8(4): 103972.

Gupta VK, Shrivastava AK and Jain N. Biosorption of chromium (VI) from aqueous solutions by green algae Spirogyra species. *Water Res.* 2011; 35(17): 4079-4085.

Jing X, Cao Y, Zhang X, Wang D, Wu X and Xu H. Biosorption of Cr (VI) from simulated wastewater using a cationic surfactant modified spent mushroom. *Desalination* 2011; 269(1-3): 120-127.

Kanamarlapudi SLRK, Chintalpudi VK and Muddada S. Application of biosorption for removal of heavy metals from wastewater. *Biosorption* 2018; 18(69): 69-116.

Khan MKA, Alam M, Islam MS, Hassan MQ and Al-Mansur MA. Environmental pollution around Dhaka EPZ and its impact on surface and groundwater. *Bangladesh J. Sci. Ind. Res*. 2011; 46(2): 153-162.

Kumari P, Sharma P, Srivastava S and Srivastava MM. Biosorption studies on shelled Moringa oleifera Lamarck seed powder: Removal and recovery of arsenic from aqueous system. *Int. J. Miner. Process*. 2006; 78(3): 131-139.

Langmuir D. Aqueous Environmental Geochemistry. Prentice-Hall. Inc., *New Jersey* 1997; p. 343-402

Lima ÉC, Adebayo MA and Machado F. Kinetic and equilibrium models of adsorption. In: Carbon Nanomaterials as Adsorbents for Environmental and Biological Applications. *Springer* 2015; p. 33-69.

Mathialagan T, Viraraghavan T and Cullimore, DR. Adsorption of cadmium from aqueous solutions by edible mushrooms (Agaricus bisporus and Lentinus edodes). *Water Qual. Res. J. Canada* 2003; 38(3): 499–514.

Michalak I, Chojnacka K and Witek-Krowiak A. State of the art for the biosorption process—a review. *Appl. Biochem. Biotechnol*. 2013; 170: 1389-1416.

Nuhoglu Y, Malkoc E, Gurses A and Canpolat, N. The removal of Cu (II) from aqueous solutions by Ulothrix zonata. *Bioresour. Technol*. 2002; 85(3): 331-333.

Papassiopi N, Vaxevanidou K, Christou, C, Karagianni E and Antipas GSE. Synthesis, characterization and stability of Cr (III) and Fe (III) hydroxides. *J. Hazard. Mater.* 2014; 264: 490-497.

Parkhurst DL and Appelo CAJ. Description of input and examples for PHREEQC version 3--a Computer program for speciation, batch-reaction, one-dimensional transport, and inverse geochemical calculations: U.S. Geological Survey techniques and methods, USGS 2013.

Prasad YL and Sachin DR. Biosorption of Cu , Zn , Fe , Cd , Pb and Ni by Non-Treated Biomass of Some Edible Mushrooms. *Asian J. Exp. Biol. Sci.* 2013; 4(2): 190-195.

Rahman MS, Saha N and Molla AH. Potential ecological risk assessment of heavy metal contamination in sediment and water body around Dhaka export processing zone, Bangladesh. *Environ. Earth Sci.* 2014; 71: 2293-2308.

Reddy DHK, Harinath Y, Seshaiah K and Reddy AVR. Biosorption of Pb(II) from aqueous solutions using chemically modified Moringa oleifera tree leaves. *Chem. Eng. J.* 2010; 162(2): 626-634.

Reddy DHK, Ramana DKV, Seshaiah K and Reddy AVR. Biosorption of Ni(II) from aqueous phase by Moringa oleifera bark, a low cost biosorbent. *Desalination* 2011; 268(1-3): 150-157.

Sabur MA. Interactions of Phosphate and Silicate with Iron oxides in Freshwater Environments. *University of Waterloo* 2019.

Sag Y and Kutsal T. Recent trends in the biosorption of heavy metals: A review. Biotechnol. *Bioprocess Eng.* 2001; 6: 376-385.

Say R, Denizli A and Arıca MY. Biosorption of cadmium (II), lead (II) and copper (II) with the filamentous fungus Phanerochaete chrysosporium. *Bioresour. Technol*. 2001; 76(1): 67-70.

Shakoor MB, Niazi NK, Bibi I, Shahid M, Saqib ZA, Nawaz MF, Shaheen SM, Wang H, Tsang DCW, Bundschuh J, Ok YS and Rinklebe J. Exploring the arsenic removal potential of various biosorbents from water. *Environ. Int*. 2019; 123: 567-579.

Suseem SR and Mary Saral A. Biosorption of heavy metals using mushroom Pleurotus eous. *J. Chem. Pharm. Res.* 2014; 6(7): 2163-2168.

Szabó M, Kalmár J, Ditrói T, Bellér G, Lente G, Simic N and Fábián I. Equilibria and kinetics of chromium (VI) speciation in aqueous solution–a comprehensive study from pH 2 to 11. *Inorganica Chim. Acta* 2018; 472: 295-301.

Uluozlu OD, Sari A, Tuzen M and Soylak M. Biosorption of Pb(II) and Cr(III) from aqueous solution by lichen (Parmelina tiliaceae) biomass. Bioresour. *Technol*. 2008; 99(8): 2972-2980.

Vimala R and Das N. Biosorption of cadmium (II) and lead (II) from aqueous solutions using mushrooms: A comparative study. *J. Hazard. Mater*. 2009; 168(1): 376-382.

Wuana RA and Okieimen FE. Heavy metals in contaminated soils: a review of sources, chemistry, risks and best available strategies for remediation. *Isrn Ecol*. 2011; ID 402647: 1-20.